Quaternary Geochronology 91 (2026) 101705

Contents lists available at ScienceDirect

Quaternary Geochronology

journal homepage: www.elsevier.com/locate/quageo

'Mammothfluidics': Amino acid dating of fossil mammal tooth enamel using a modular microfluidic system

Laila Patinglag [a], Marc R. Dickinson [b], Marcus Hill [a], Kirsty E.H. Penkman [b], Kirsty J. Shaw [a,*]

[a] Department of Natural Sciences, Manchester Metropolitan University, Manchester, M1 5GD, UK
[b] Department of Chemistry, University of York, York, YO10 5DD, UK

ARTICLE INFO

Keywords:
Microfluidics
Amino acid racemisation
Racemisation
Pleistocene

ABSTRACT

Dating fossil samples helps reconstruct evolutionary history, aiding conservation efforts and mitigating climate change impacts. Amino acid geochronology of tooth enamel using the intra-crystalline protein decomposition (IcPD) approach allows direct dating of mammal teeth over Quaternary timescales (~2.5 million years), beyond the limits of radiocarbon dating (~50,000 years). However current methods require specialist equipment and relatively lengthy processing times. We developed a modular microfluidic system for chiral amino acid analysis of tooth enamel samples, consisting of three sequential glass microfluidic devices for sample bleaching, release of hydrolysable amino acids, and biphasic separation. Relative concentrations and D/L values of key amino acids were measured using reverse-phase high performance liquid chromatography (RP-HPLC). The microfluidic method reduced sample amounts from ~15 mg to ~1 mg and bleaching time from 72 h to 2 h. Amino acid compositions of modern and fossil samples were similar between the microfluidic approach and standard IcPD method, with good agreement up to D/L values ~0.5 for phenylalanine (Phe) and glutamic acid (Glx). The method worked successfully across various genera and operators, with reduced sample mass and analysis time. This approach results in less destructive sampling of precious fossil samples and enables preparation steps in non-specialist labs, potentially allowing IcPD dating within the fossils' country.

1. Introduction

Dating fossil samples is critical for the reconstruction of evolutionary history, helping us to understand biotic responses to climatic conditions that can also aid with modern conservation efforts and mitigate the impact of climate change (Fordham et al., 2020). Amino acid geochronology using the intra-crystalline protein decomposition (IcPD) approach allows direct dating of biominerals in temperate regions over at least Quaternary timescales (~2.5 million years). IcPD dating measures the chiral amino acid composition trapped within the intra-crystalline fraction of fossil samples, and therefore protected from the external chemical environment for the duration of diagenesis. The development of the approach for tooth enamel (Dickinson et al., 2019) has enabled direct dating of mammalian fauna (Dickinson et al., 2024), as well as evidence for palaeoproteomic endogeneity (e.g. Cappellini et al., 2019; Paterson et al., 2024), but current methods rely on specialist laboratory equipment, sample masses of ~15 mg, and relatively lengthy processing times (Dickinson et al., 2019).

Microfluidics enables the performance of laboratory processes on a miniaturised scale (Whitesides, 2006). By miniaturising these processes, advantages are afforded in terms of high surface area to volume ratios, which can lead to faster reaction times and increased efficiencies. In particular, it enables the use of smaller sample sizes, useful for example when examining rare or difficult to obtain material, in this case where smaller and/or more precious archaeological samples can be examined. Microfluidics can also be used to integrate multiple techniques into a single 'lab-on-a-chip', enabling movement from one process to the next whilst minimising the risk of sample loss or contamination ((Li et al., 2021)). This is important when dealing with precious archaeological or palaeontological samples; for example we have previously demonstrated the use of microfluidics for biological sex estimation using ancient DNA from human remains, with minimal sample requirements enabling repeat analysis (Parton et al., 2012). There are many other examples in the literature demonstrating DNA analysis in integrated microfluidic systems (Li et al., 2021; Yin et al., 2019), but less on the analysis of amino acids as another key biomarker, and none for chiral amino acid analysis from biominerals.

Microfluidic amino acid analysis has previously focussed on sample

* Corresponding author.
E-mail address: k.shaw@mmu.ac.uk (K.J. Shaw).

https://doi.org/10.1016/j.quageo.2025.101705
Received 21 May 2025; Received in revised form 5 September 2025; Accepted 6 September 2025
Available online 12 September 2025

preconcentration, pre- and post-column derivatisations, and detection (Pumera, 2007). Key challenges were identified including low target analyte concentration, a lack of research demonstrating use of real-world samples for analysis and the difficulties in creating effective 'world-to-chip' interfaces. Since then researchers have shown, for example, microfluidic devices manufactured from paper which are able to quantify single (Santhosh and Park, 2022) or multiple amino acids (Kugimiya et al., 2022) using colourimetric methods. However, for dating purposes we require not just amino acid concentration but also a thorough understanding of the D/L values, as racemisation is a key diagenetic reaction in amino acid geochronology. Microfluidic capillary electrophoresis devices coupled with laser-induced fluorescence for chiral separation of amino acids have been shown to be beneficial, for example in space exploration, due to their low instrument mass and minimal sample requirements (Pietrogrande, 2013). Despite this, fully integrated microfluidic systems which are capable of accepting real-world samples for chiral amino acid analysis have not been explored, yet offer great potential.

Here we develop and test a modular microfluidic approach to amino acid dating, using sample bleaching to isolate the intra-crystalline amino acids from tooth enamel and combining this with release of hydrolysable amino acids and biphasic separation to remove phosphate ions, before conventional reverse phase-high performance liquid chromatography (RP-HPLC) analysis. Optimisation of the three different preparation steps (bleaching, hydrolysis and biphasic separation) is presented, alongside comparison of the integrated system with conventional preparation methods.

2. Experimental

2.1. Sample collection and preparation

Enamel samples were obtained from teeth of a range of commonly-occurring Quaternary taxa and levels of degradation (Table 1).

Table 1
Sample information for enamel specimens. *To provide a consistent comparator, the level of degradation was defined by total hydrolysable amino acid fraction (THAA) Glx D/L values: low ≤0.10, medium 0.11–0.40, high ≥0.40

Taxonomy	Name	Location	Age	Level of amino acid degradation*
Alcelaphini	ZaTwAlE28.3	Twin Rivers, Zambia	Pleistocene	Medium
Bovidae	SAKrBE9b1	Kromdraai, South Africa	2.0–1.6 Ma	High
Ceraotherium simum	ZaTwRhE20.5	Twin Rivers, Zambia	Pleistocene	Medium
	TWSIE1.4.B	Twin Rivers, Zambia	Pleistocene	High
Elephas maximus	MoEE	NA	Modern	Low
Equus ferus	MoEqE	NA	Modern	Low
Equus sp.	ZaTwEqE12.1	Twin Rivers, Zambia	Pleistocene	High
	TWEQE24.2.B	Twin Rivers, Zambia	Pleistocene	High
Mammalia	SAPP23b1	Pinnacle Point, South Africa	170–40 ka	Low
Mammuthus primigenius	TaME	Tattershall, UK	~160 ka	Low
Mammuthus trogontherii	WiME	Witham, UK	~500 ka	Low
Palaeoloxodon antiquus	SwPE2	Swanscombe, UK	~374 ka	Low
	ItLPPE3	La Polledrara, Italy	~337 ka	Medium
Phacochoerus sp.	MCPHE4.B	Mumbwa Caves, Zambia	>172 ka	Medium

Following the methods of Dickinson et al. (2019), a chip of enamel was extracted from each tooth, and any adhering dental tissues (e.g. dentine and cementum) were carefully removed using a precision drill fitted with a diamond-coated abrasive cutting disc. The outer enamel surface was removed using a diamond-coated burr (typically a 2 mm ball or flame-shaped bit). The enamel was then rinsed with deionised water, left to air dry overnight in a sterile loosely covered plastic microcentrifuge tube (Eppendorf) and powdered using an agate pestle and mortar.

2.2. Conventional IcPD preparation

In order to evaluate the module microfluidic approach, samples were analysed in parallel using the conventional IcPD dating method developed by Dickinson et al., (2019). The current technique for amino acid analysis in enamel combines RP-HPLC (Kaufman and Manley, 1998) with the isolation of the intra-crystalline amino acid fraction via sodium hypochlorite (bleach) treatment (Penkman et al., 2008; Sykes et al., 1995). This methodological combination enables the determination of D/L values of multiple amino acids from the chemically protected 'closed system' protein fraction within the biomineral. This enhances analytical reliability while reducing required sample mass. Sample preparation followed optimised procedures for enamel, including a 72-h bleach treatment to isolate the intra-crystalline protein fraction. Samples were subjected to acid hydrolysis to release peptide-bound amino acids, yielding the total hydrolysable amino acid fraction (THAA, denoted H). Following enamel demineralisation, the pH of the resulting solution was adjusted with KOH and centrifuged at 13,000 rpm for 5 min, producing a biphasic solution. The supernatant was extracted and dried via centrifugal evaporation.

2.3. Modular microfluidic IcPD preparation

A modular approach to the preparation of enamel samples for IcPD analysis was taken, in which microfluidic devices were individually designed for the bleaching, hydrolysis and biphasic separation steps. Fabrication and method optimisation are described, before the microfluidic devices were run in series to prepare samples and compare to conventional methods (see Section 2.2).

2.3.1. Microfluidic device design and fabrication

Microfluidic devices were designed in AutoCAD and the microchannels were drilled onto 1 mm glass bottom plates (Schott B270, Tellic, USA) using a Computer Numerical Control (CNC) machine (Datron, UK). Three different designs were produced, one for each of the preparation steps: bleaching (1), hydrolysis (2) and biphasic separation (3). 1) For bleaching, the design consisted of a single 150 μm depth channel (Fig. 1a) with a 100 μm height weir to enable packing of enamel (Fig. 1b); 2) For hydrolysis, the device contained a single 40 μL reaction chamber (Fig. 1c); 3) for biphasic separation, a single 150 μm depth channel with 2 inlets and 3 outlets was used (Fig. 1d). Both inlet and outlet holes [1/16″ outer diameter (OD)] were drilled through a 3 mm thick glass top plate (Schott B270, Tellic, USA), aligned with the drilled glass bottom and thermally bonded by heating in a furnace. Fluorinated ethylene propylene (FEP) tubing [1/16″ OD × 0.030″ inner diameter (ID)] (Cole-Palmer, UK) was glued, using Araldite two-part epoxy adhesive (Huntsman Advance Materials, UK), to the glass devices and interfaced using adapters and connectors (Cole-Palmer, UK) to BD Luer-lock syringes (Fisher Scientific, UK). The operation of each individual microfluidic device was optimised and then combined in a modular set-up as outlined in Fig. 1e.

2.3.2. Bleaching

Prior to loading on to the first microfluidic device, powdered samples were sieved to ensure a more uniform particle size distribution and prevent blocking. A range of different filter sizes (40, 60, 85 and 100 μm (Cambridge Bioscience, UK)) were used with modern (*E. maximus*) and

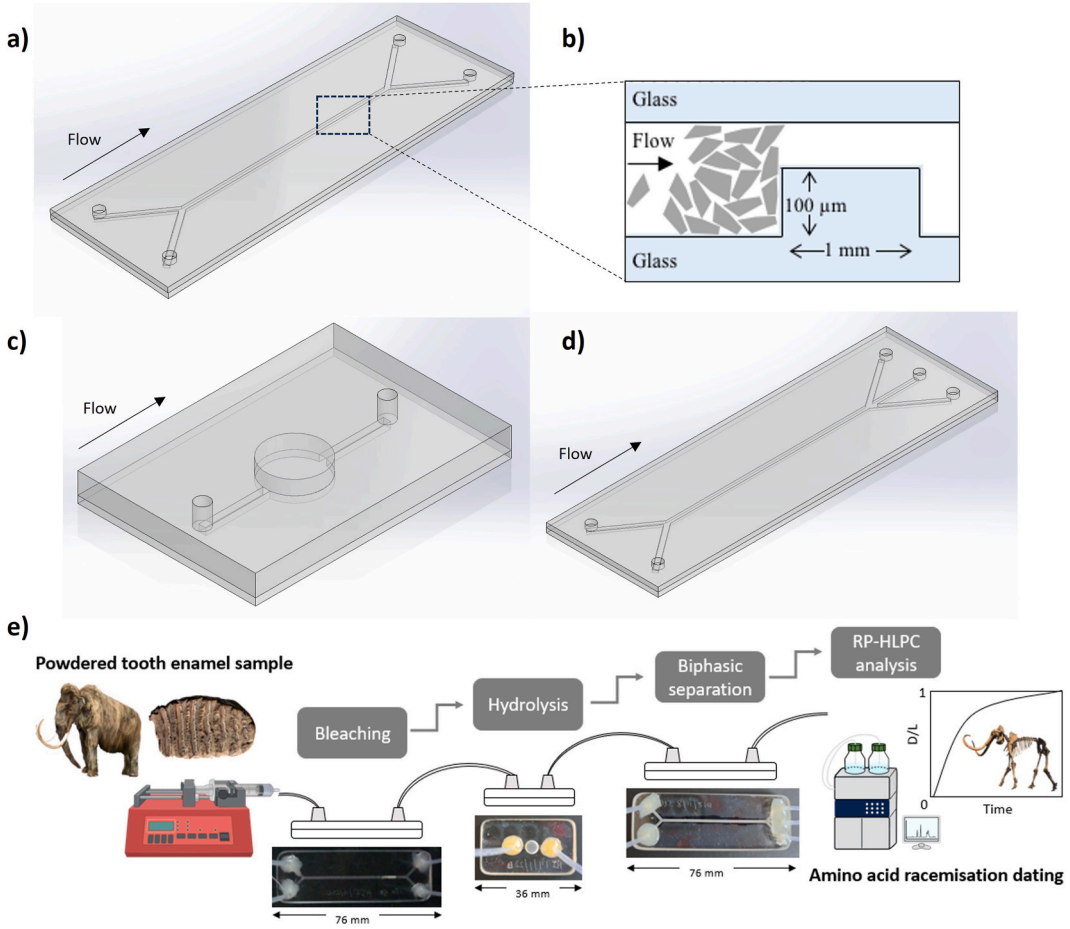

Fig. 1. CAD images of the microfluidic devices used for a) bleaching of enamel samples including b) cross-section of the weir design feature, c) hydrolysis, d) biphasic separation, and e) schematic showing the modular microfluidic approach to IcPD of powdered enamel samples prior to RP-HPLC analysis.

older (*M. trogontherii*) samples, and particle size distribution evaluated using scanning electron microscopy (SEM, Supra 40VP with SmartSEM software (Carl Zeiss Ltd. UK)).

The powdered samples (~2 mg) were then mixed with HPLC grade water (1 mL/mg) to create a slurry and injected into the microfluidic device (Fig. 1a). Sodium hypochlorite (12 %, VWR, UK) was pumped through the device at a flow rate of 30 µL/min controlled via syringe pump (Cronus Sigma, 2000C, SMI-LabHut Ltd., UK) and ran for various times between 1 and 24 h. The treated sample was rinsed using HPLC grade water at 30 µL/min for 10 min. Collected liquid from the outlet was tested using litmus paper for residual sodium hypochlorite in the device. HPLC grade methanol was then pumped at 30 µL/min flow rate for 5 min and the samples dried by pumping air over.

2.3.3. Hydrolysis

Bleached samples were dissolved by flowing 7 M HCl (Sigma-Aldrich, UK) at 10 µL/min for 4 min through the device to demineralise the samples. These samples were then transferred to a second microfluidic device (Fig. 1c) which had previously been flushed with nitrogen. Once the chamber was filled, the inlet and outlet were sealed and the samples heated in the oven at various temperature between 50 °C and 95 °C, over 1–24 h to generate the total hydrolysable amino acids (THAA). Following heating, samples were dried overnight at 30 °C.

2.3.4. Biphasic separation

The final microfluidic device (Fig. 1d) required silanisation prior to use to achieve a stable laminar flow regime. The device was cleaned with sequential washes of 1 M sodium hydroxide (Alfa Aesar, UK), HPLC grade water and ethanol (VWR, UK) at 5 µL/min for 30 min each, then left to dry at 90 °C. The microchannels were then coated using Sigma-Cote (Sigma-Aldrich, UK) at 5 µL/min for 5 min, before the devices were washed sequentially with acetone and water for 5 min each at 5 µL/min. Following silanisation, 20 µL/mg of 1 M HCl was added to the dried samples (Section 2.3.3.) and flowed into the device from the top inlet. Next, 28 µL/mg of 1 M potassium hydroxide (Fisher Scientific, UK) was simultaneously flowed through the bottom inlet at 3 µL/min. The resulting laminar flow enabled gel formation at the interface, and the supernatant to be collected from the outlet before being dried overnight at room temperature.

2.4. Reverse phase – high performance liquid chromatography (RP-HPLC)

The dried-down samples were rehydrated with a solution containing 0.01 mM L-homo-arginine as an internal standard, and then analysed using RP-HPLC to enable the relative concentrations and D/L values of a series of amino acids to be measured (Dickinson et al., 2019). During preparative acid hydrolysis, asparagine (Asn) and glutamine (Gln) irreversibly deaminate to aspartic acid (Asp) and glutamic acid (Glu), respectively. As such, these are reported collectively as Asx (Asp + Asn) and Glx (Glu + Gln). D/L values were then compared for key amino acids, namely Asx, Glx, alanine (Ala) and phenylalanine (Phe), as their breakdown patterns are predictable and both their D and L peaks can be well resolved in enamel by RP-HPLC (Dickinson et al., 2019) Data analysis and production of figures was carried out in Excel, GraphPad and R studio. A two-way ANOVA was used to compare D/L values

obtained by the microfluidic and conventional methods, and a paired *t*-test was used to compare results from different microfluidic device operators.

3. Results & discussion

3.1. Sample filtering

Filtering of the samples is essential to ensure efficient packing of the microfluidic device for the bleaching step and to prevent blockages. A range of filters were evaluated, ranging from 40 to 100 μm, and the results showed that the use of a 40 μm filter produced consistent size particles for both modern (Fig. 2a) and fossil (Fig. 2b) samples. These particles were able to create the desired keystone effect, facilitated through inclusion of a weir structure within the microfluidic device, alongside a high surface area for fluid interaction. Previous studies have shown how weir, tapered and bottleneck channels can be used to retain particles of various sizes, but they predominantly feature spherical shaped samples in achieving the keystone effect (Vanapalli et al., 2008). In this study, the particles are predominantly elongated rectangular or irregular shapes (Fig. 2c and d) which can affect parameters such as void spaces between particles, surface area and fluid dynamics. By using a longer channel with reduced depth, this can increase the number of voids in the sample bed, reducing hydrodynamic resistance and unwanted pressures within the device (De Pra et al., 2008). This channel design enabled packing of ~1 mg of enamel sample (Fig. 2e shows a photograph of a packed device), a reduction in sample size compared with the ~15 mg used in conventional IcPD analysis (Dickinson et al., 2019).

3.2. Bleaching step

The effect of bleaching time was examined for *M. trogontherii, M. primigenius* and *E. ferus* (representing a wide range of sample ages) within the microfluidic device and compared with conventional preparation. Amino acid D/L values increased after 1 h of bleach treatment for both *M. trogontherii* (Fig. 3a) and *M. primigenius* (Fig. 3b) and plateaued after 2 h of exposure, indicating isolation of the intra-crystalline fraction of amino acids. This decrease in bleaching time compared with the conventional IcPD preparation (72 h bleaching time) is as a result of the high surface area to volume ratio created by use of the microfluidic device, enabling more efficient interaction of the bleach with the enamel in a continuous flow environment (Manz et al., 2020).

A bleaching time of 2 h was therefore used for subsequent analyses of the modern horse (*E. ferus*). A significant decrease in the concentration of all amino acids was observed using the microfluidic method, resulting in similar concentrations (within 1 standard deviation) to the 72 h conventional method, which corresponds to the removal of inter-crystalline amino acids and isolation of the intra-crystalline amino acids. Gly is a common contaminant due to its high relative concentration in collagen (dentine) and in lab processes, but the microfluidics method greatly reduces the Gly concentration. The microfluidics variability within samples is generally slightly higher than the conventional method, likely as a result of the smaller sample masses analysed.

The effect of bleaching was also examined on equid samples as another species model (Fig. 3c and d) which showed that a 2 h heating time also produced the highest concentration of amino acids. However, it was observed that over longer heating periods the amino acid concentrations decreased, with potentially negative effects on the sample as the mineral can start to be etched away (Dickinson et al., 2019). In all subsequent experiments, using any species, a 2 h bleaching step was therefore used.

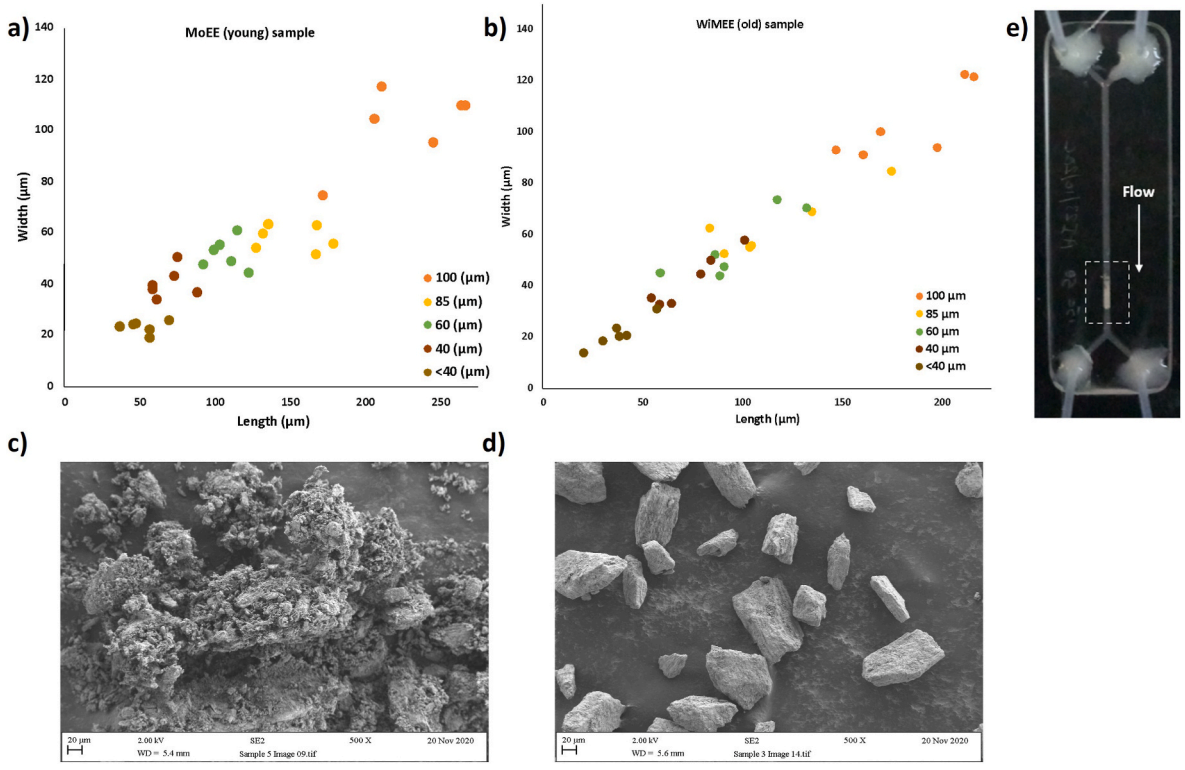

Fig. 2. Particle size distribution following filtering for both **a)** modern, and **b)** fossil enamel samples. SEM images showing **c)** unfiltered samples had a combination of distinctive shaped particles and fine powders, whereas **d)** filtered samples were more regular in their size and shape distribution; **e)** photograph showing packing of the enamel against the weir in the microfluidic channel.

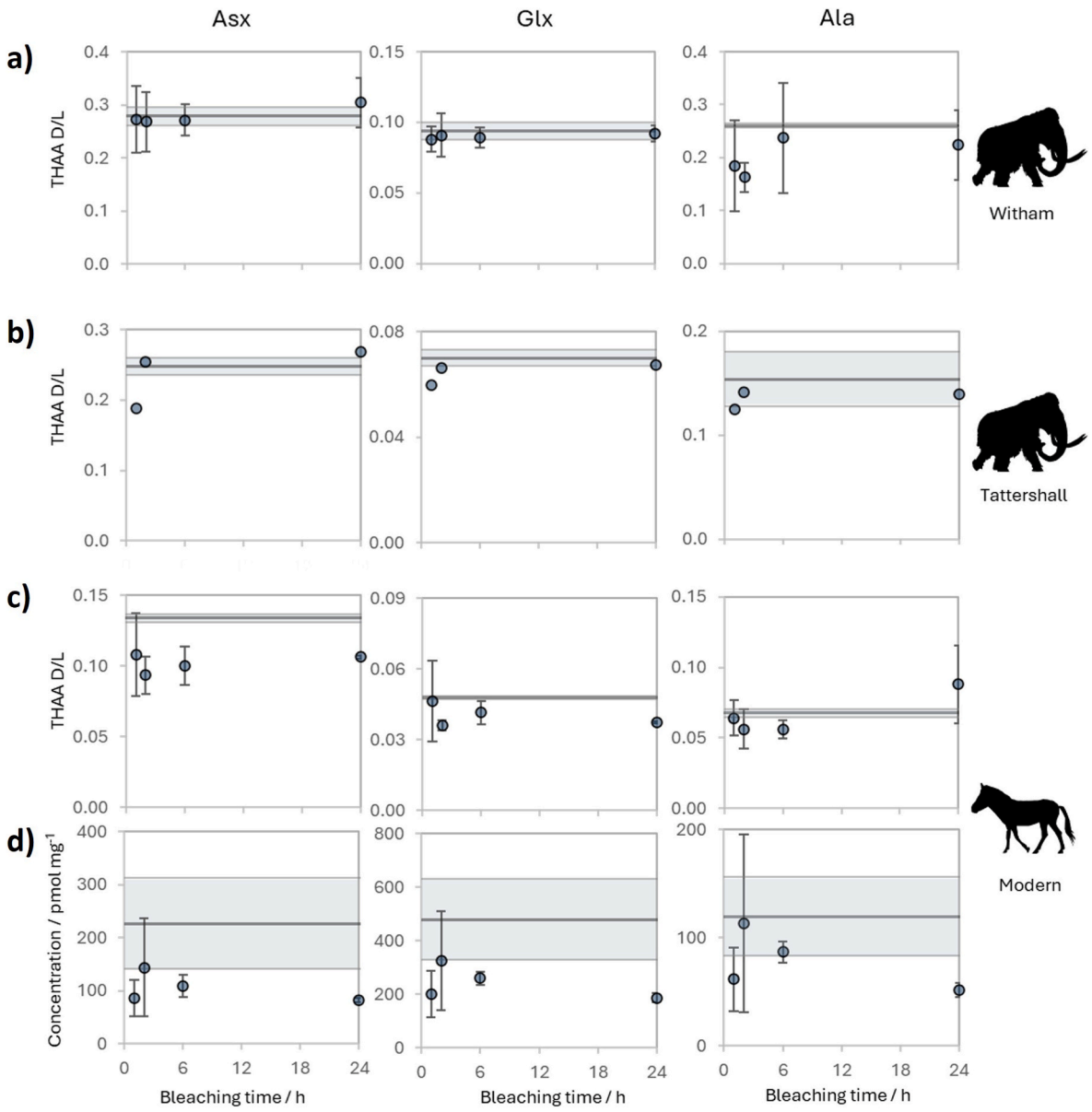

Fig. 3. *THAA D/L values (a, b and c) and concentrations (d) for key amino acids, Asx (left), Glx (middle), and Ala (right), after microfluidic bleach treatment of* M. trogontherii *from Witham (top row),* M. primigenius *from Tattershall (top-middle row), and modern* E. ferus *(bottom two rows) samples for various bleaching times up to 24 h (n=3). The blue shading represents the mean and standard deviation of the same samples processed using conventional IcPD method of bleaching the sample for 72 h.*

3.3. Hydrolysis step

3.3.1. Effect of temperature

The effect of different hydrolysis temperatures within the microfluidic device were evaluated for the oldest *M. trogontherii* samples. For the intra-crystalline amino acids isolated after bleach treatment, the D/L values of amino acids increased with increasing temperatures up to 95 °C (Fig. 4). Higher temperatures (100 °C and above) were also tested within the microfluidic device, but there were practical challenges in ensuring the sample stayed contained within the system, and high losses were observed. Concentrations and D/L values reached using the microfluidic at 95 °C for hydrolysis were within the standard deviation of results using the conventional method at 110 °C, with the exception of lower D/L values observed with Phe.

3.3.2. Effect of different heating times

Once the optimal temperature had been established (95 °C), the effect of different heating times on hydrolysis was evaluated. In the *M. trogontherii* samples, D/L values for the key amino acids increased after 1 h, and then plateaued after 2 h (Fig. 5a). However, a plateau was not observed with the total amino acid concentrations after 2 h of heating (Fig. 5b), with [THAA] gradually increasing with heating time up to 24 h. *E. ferus* samples were also evaluated to ensure the proposed microfluidic hydrolysis treatment worked across different taxa. The amino acid concentrations were found to increase over time and, with the exception of Phe which tends to be poorly resolved, were comparable with the conventional IcPD methodology (Fig. 5c). Overall, the results indicated that hydrolysis conditions for 95 °C for 24 h was optimal in the microfluidic system, and these conditions were used in all subsequent experiments.

3.4. Biphasic separation step

If excess phosphate ions are not removed from the hydrolysed samples, peak suppression (indicated by reduced internal standard peak area) occurs (Dickinson et al., 2019), resulting in poor quality

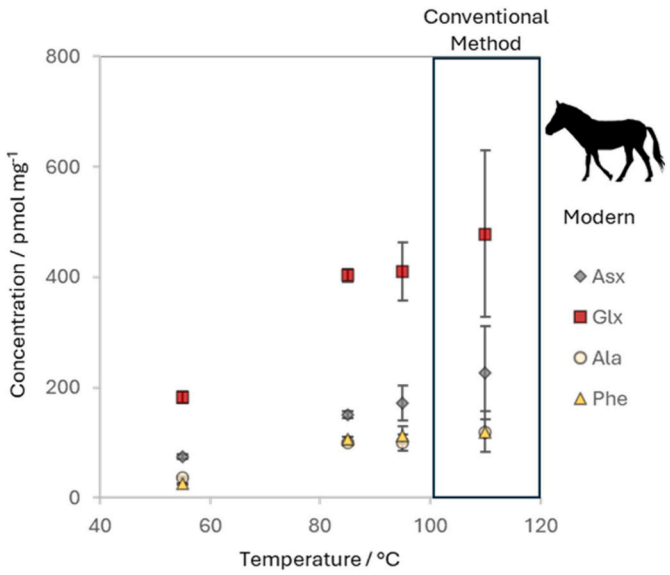

Fig. 4. Concentration of key amino acids (Asx, Glx, Ala and Phe) hydrolysed at various temperatures for 24 h (n = 3). The concentration increases with temperature up to 95 °C, with release of free amino acids by peptide bond hydrolysis; at higher temperatures evaporation and degradation reduces the amino acid concentration.

chromatographs and poorer quantification. In the conventional preparation, hydrolysed samples are treated with potassium hydroxide producing a biphasic solution from which the supernatant is extracted. In the microfluidic device, the aim was to replicate this using laminar flow of the solutions, enabling gel formation to occur at the interface, followed by separation of the gel and supernatant through different outlets. The biphasic separation experiments revealed the importance of silanisation of the microfluidic device, ensuring consistent laminar flow to enable gel formation at the interface of the hydrolysed samples with potassium hydroxide (example images are shown in Fig. 6a), as well as producing high quality chromatograms (Fig. 6b). The concentration of the total hydrolysable amino acids were found to be slightly lower (Fig. 7a) and D/L values slightly higher using the microfluidic device than the conventional method (Fig. 7b). However, two-way ANOVA on those D/L values found no significant differences between methods ($F(1,20) = 0.7640$, $DF = 1$, $P = 0.3925$) and no significant interaction between method and amino acid ($F(3,20) = 0.06961$, $DF = 3$, $P = 0.9755$).

3.5. Integrated modular analysis

Following optimisation of the individual microfluidic devices associated with each phase of analysis, samples from a range of ages and taxa were prepared using the combined microfluidic modules (run in series) and results compared with the conventional IcPD method. The relative composition of hydrolysable amino acids obtained by the two methods showed good correspondence (Fig. 8). Amino acid concentrations in enamel were typically in the range of approximately 10–1000 pmol mg^{-1}. The agreement between the extents of racemisation across the

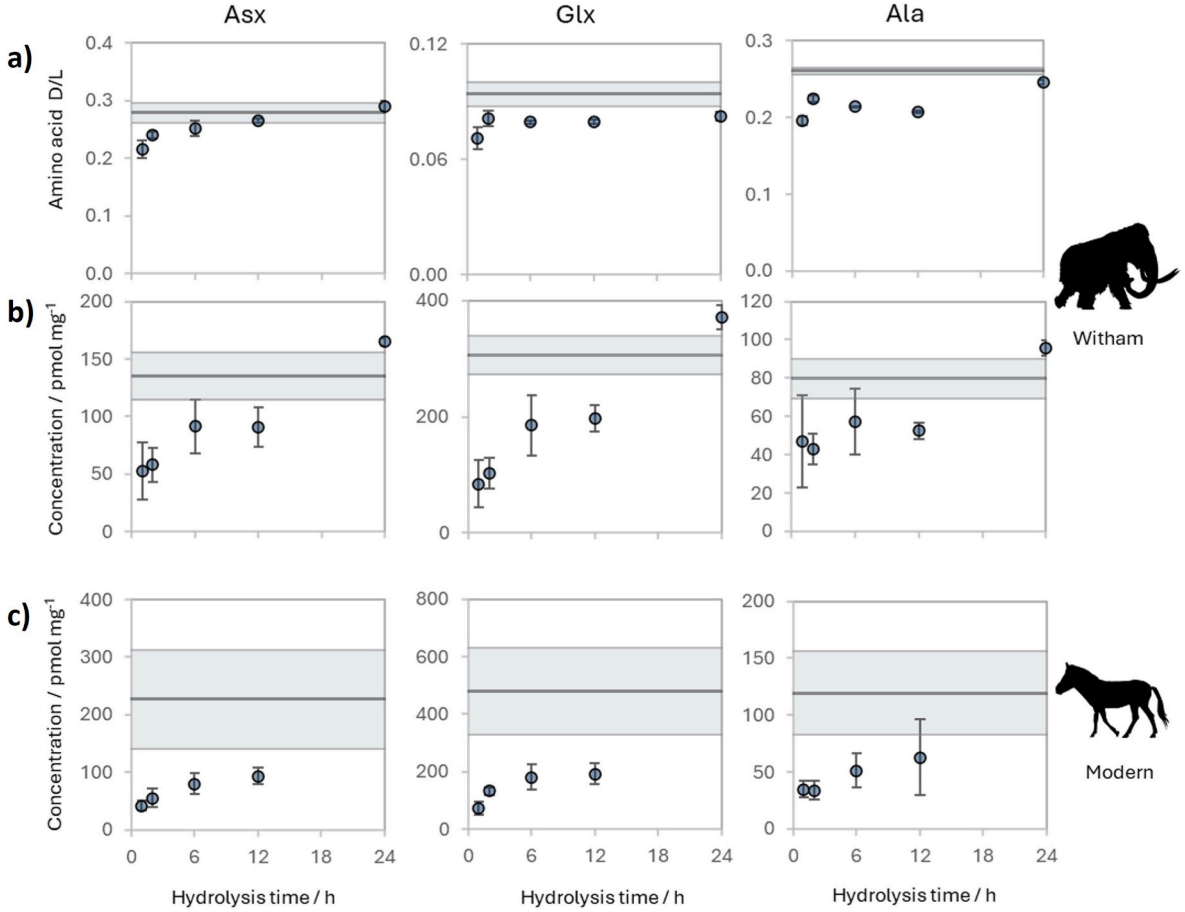

Fig. 5. *D/L values (a) and concentration (b and c) for key amino acids, Asx (left), Glx (middle), and Ala (right), with different incubation times for hydrolysis of* M. trogontherii *enamel from Witham (a and b) and* E. ferus *(c) at 95°C (n=3). The blue shading represents the mean and standard deviation for the conventional IcPD method of hydrolysing samples at 110°C for 24 h. After 6 h the D/Ls remain stable, indicating continued hydrolysis up to 24 h does not cause significant degradation.*

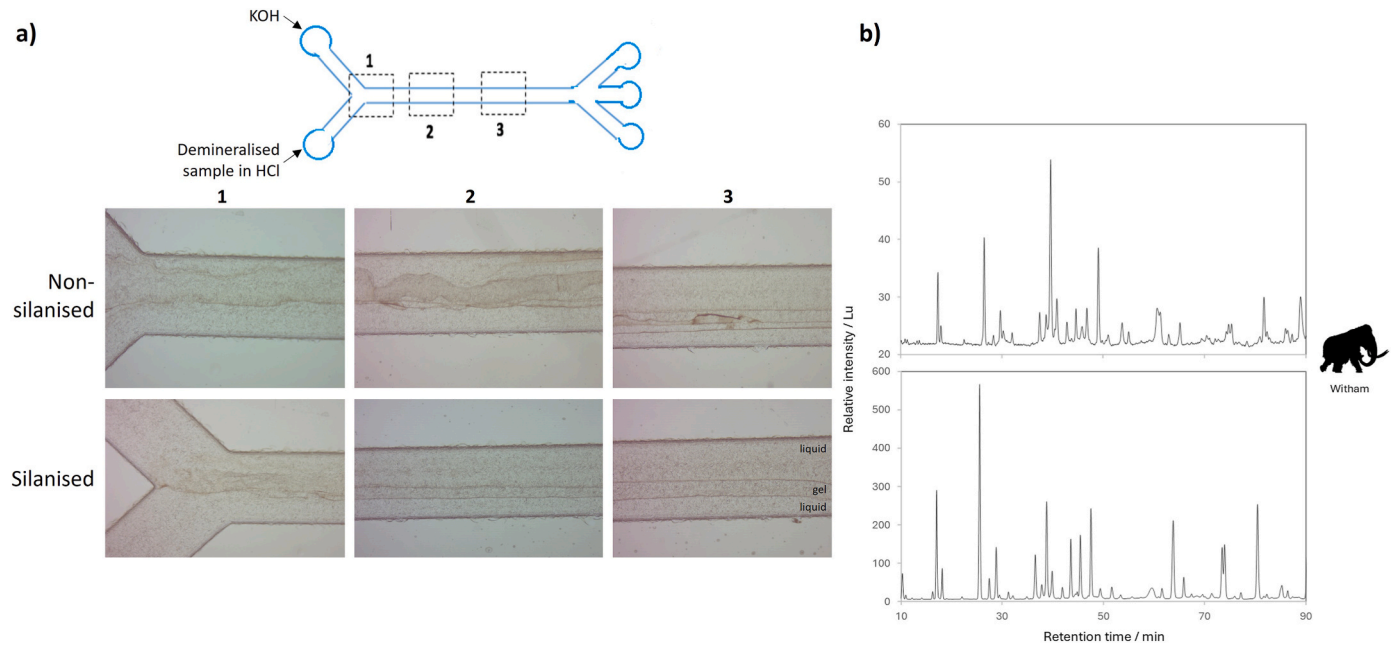

Fig. 6. *a) Example bright-field microscope images showing gel formation at locations 1, 2 and 3 in non-silanised (top) and silanised (bottom) channels, with laminar flow regimes clearly visible in the silanised channels. b) HPLC chromatograms (fluorescence detection, relative intensity in luminescence units (Lu)) of chiral amino acids extracted from a* M. trogontherii *tooth from Witham. The non-silanised channels resulted in lower relative intensities and a noisy baseline, which complicates accurate peak area determination (top). Silanised channels exhibiting higher relative intensity and a cleaner baseline, allowing for more precise and reliable integration of amino acid peaks (bottom).*

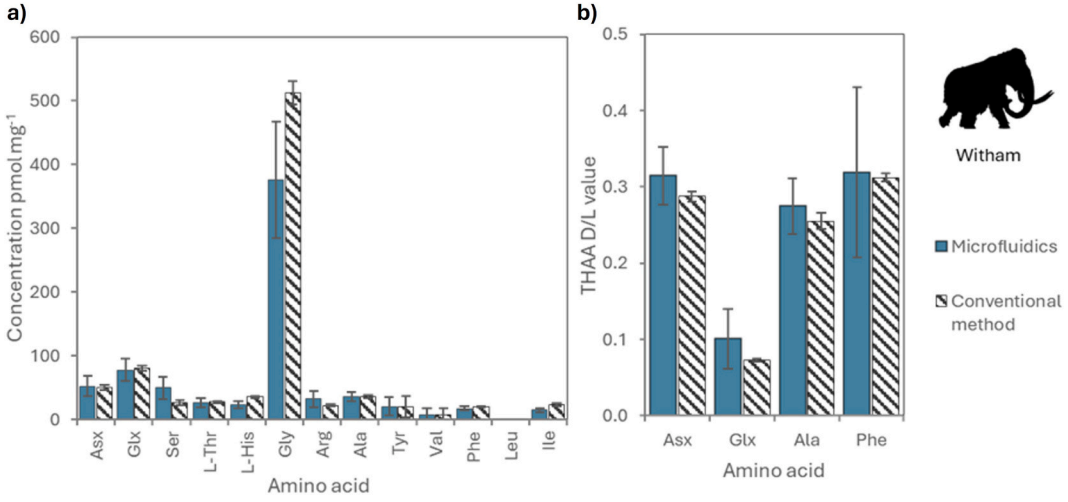

Fig. 7. a) *Amino acid composition of the* M. trogontherii *sample in the supernatant layer using a microfluidic device compared with the conventional IcPD preparation;* ***b)*** *D/L value of the amino acids in the supernatant layer using a microfluidic device compared with the conventional preparation ($n \geq 3$).*

methods was most robust for Glx and Phe, with D/L values closely matching and showing average deviations of ±0.02 for Phe and ±0.05 for Glx up to ~0.5. In contrast, the correlation was slightly higher for Asx and Ala, with average deviations of ±0.06 for Asx D/L values and ±0.08 for Ala for values up to 0.5. These values take us back to a conservative estimate of approximately 1 Ma in northern Europe (Dickinson et al., 2024) and the Middle Pleistocene in southern Africa (Baldreki et al., 2024; Politt et al., 2025) (current mean surface temperature of ~18–25 °C), after which the microfluidics method produced consistently lower values than the conventional method (Fig. 9). The microfluidic preparation method was shown to work successfully up to D/Ls ~0.5 across the range of taxa examined (bovids, elephantids, equids, rhinocerotids and suids; Fig. 9). In order for the microfluidic system to be of value, it also needs to produce consistent results across different operators; in this study two different operators analysed a range of samples across taxa and levels of degradation. Results from each operator had similar trends compared with the conventional method, and analysis of a number of replicate samples showed no statistical differences between the two operators ($t(2) = 1.105$, $p = 0.3844$, two-tailed) (Fig. 9).

4. Conclusions

A novel modular microfluidic system has been demonstrated for amino acid dating using the IcPD approach, combining sample bleaching, hydrolysis and biphasic separation. The relative composition of hydrolysable amino acids obtained following optimisation of the system showed good similarity with the conventional IcPD method. Good

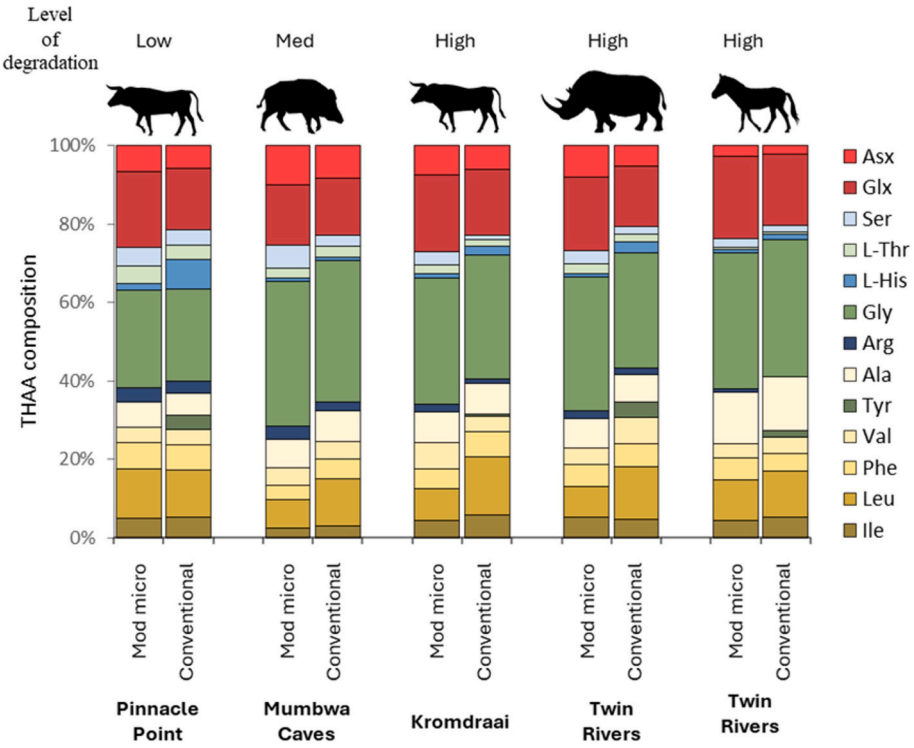

Fig. 8. Relative composition of THAA from paired samples analysed using the modular microfluidic preparation method (mod micro; left) and the conventional preparation method (right).

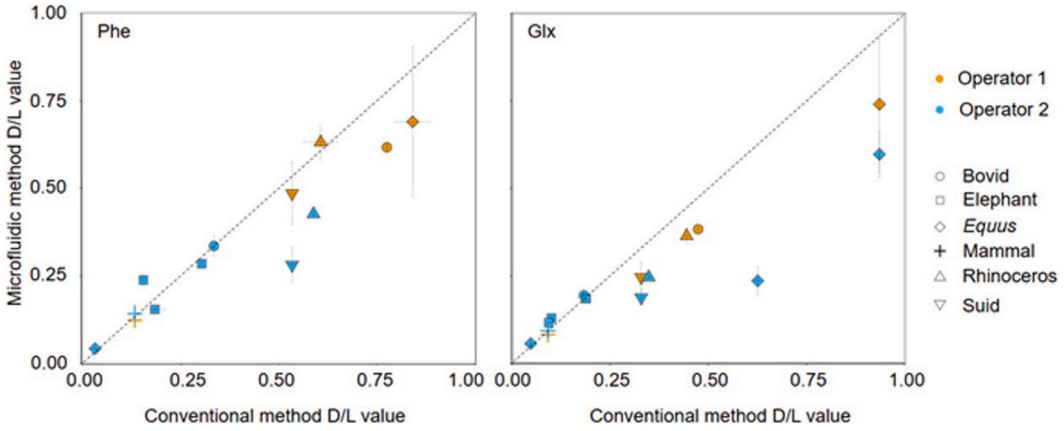

Fig. 9. Comparison of D/L values in tooth enamel of key amino acids (Phe and Glx) comparing the microfluidic method and conventional IcPD method of preparation (n = 3) for fossil samples from different genera and operators (1 and 2). The dashed line represents a 1:1 relationship; samples with D/Ls < 0.5 show good consistency between the two preparation approaches. At higher levels of degradation, the microfluidic approach results in lower D/Ls than the conventional method.

agreement between the methods was evident up to D/L values around 0.5 for the key amino acids phenylalanine (Phe) and glutamic acid (Glx). The microfluidic method was shown to work successfully across the wide range of genera tested, and between different operators. This proof-of-principle study therefore provides the first steps in a microfluidic approach for amino acid geochronology, with the optimised system enabling both sample mass and preparation time to be reduced. Further work is required to integrate microfluidic RP-HPLC analysis (or an alternative analytical method such as the use of a pillar array column (Song et al., 2013)), and understand the reasons for the disparity between the conventional and microfluidic approaches at D/L values greater than 0.5. A fully integrated 'sample in-answer out' device has huge potential to change the way Pleistocene sites are dated, for example enabling sample analysis onsite to enable chronologies to be developed while excavations continue. However by miniaturising the sample preparation steps, the advances made in this paper enable sample preparation to be undertaken outside specialist labs for the first time (meaning fossils need not be exported for analysis). This provides a first step towards enabling chronologies to be developed while excavations are still ongoing, as well as providing a less destructive sampling procedure for precious fossil enamel samples.

CRediT authorship contribution statement

Laila Patinglag: Methodology, Investigation, Formal analysis. **Marc R. Dickinson:** Writing – original draft, Visualization, Validation, Formal analysis. **Marcus Hill:** Investigation. **Kirsty E.H. Penkman:** Writing – review & editing, Visualization, Supervision, Project administration, Funding acquisition, Conceptualization. **Kirsty J. Shaw:** Writing – original draft, Supervision, Methodology, Funding acquisition,

Conceptualization.

Declaration of competing interest

The authors declare that they have no known competing financial interests or personal relationships that could have appeared to influence the work reported in this paper.

Acknowledgements

This work was primarily funded by a Natural Environment Research Council grant (NE/S010211/1), with contributions the NERC ACCE DTP (NE/S00713X/1) and the EQuaTe project that has received funding from the European Research Council (ERC) under the European Union's Horizon 2020 research and innovation programme (grant agreement No. 865222). The authors would like to thank Iek Cheong Lam (Manchester Metropolitan University) for his assistance with preparing samples for analysis, Dr Alex Iles (University of Stockholm) for manufacture of the microfluidic devices, Dr. Sam Greeves & Sheila Taylor for technical support in the NEaar lab. We would like to thank Livingstone Museum, British Geological Survey and the Zambian National Heritage Conservation Commission, Prof. Larry Barham, Prof. Curtis Marean. Prof. Adrian Lister, Dr Chloë Baldreki, Dr Bernhard Zipfel, Prof. José Braga and Dr Victoria Herridge for their support in accessing some of the samples used in this study. We would also like to thank the University of Witwatersrand and South African Heritage Resources Agency for support and access to samples from Kromdraai and Pinnacle Point used in this study.

Appendix A. Supplementary data

Supplementary data to this article can be found online at https://doi.org/10.1016/j.quageo.2025.101705.

Data availability

For the purpose of open access, the authors have applied a Creative Commons Attribution (CC BY) licence to any Author Accepted Manuscript version arising from this submission. Data in this study has been included in the supplementary information and will be available on the NOAA data repository upon publication: https://www.ncei.noaa.gov/pub/data/paleo/aar/. The Zambian teeth/fragments sampled in this study will be archived in Livingstone Museum, Zambia.

References

Baldreki, C., Dickinson, M., Reynolds, S., White, T.S., Barham, L., Penkman, K., 2024. Old fossils, new information: insights into site formation processes of two Pleistocene cave sequences in Zambia from enamel amino acid geochronology. Open Quat 10 (4), 1–17.

Cappellini, E., Welker, F., Pandolfi, L., Ramos-Madrigal, J., Samodova, D., Rüther, P.L., Fotakis, A.K., Lyon, D., Moreno-Mayar, J.V., Bukhsianidze, M., Rakownikow Jersie-Christensen, R., Mackie, M., Ginolhac, A., Ferring, R., Tappen, M., Palkopoulou, E., Dickinson, M.R., Stafford, T.W., Chan, Y.L., Götherström, A., Nathan, S.K.S.S., Heintzman, P.D., Kapp, J.D., Kirillova, I., Moodley, Y., Agusti, J., Kahlke, R.-D., Kiladze, G., Martínez-Navarro, B., Liu, S., Sandoval Velasco, M., Sinding, M.-H.S., Kelstrup, C.D., Allentoft, M.E., Orlando, L., Penkman, K., Shapiro, B., Rook, L., Dalén, L., Gilbert, M.T.P., Olsen, J.V., Lordkipanidze, D., Willerslev, E., 2019. Early Pleistocene enamel proteome from dmanisi resolves stephanorhinus phylogeny. Nature 574, 103–107.

De Pra, M., Kok, W.T., Schoenmakers, P.J., 2008. Topographic structures and chromatographic supports in microfluidic separation devices. J. Chromatogr. A 1184, 560–572.

Dickinson, M.R., Lister, A.M., Penkman, K.E.H., 2019. A new method for enamel amino acid racemization dating: a closed system approach. Quat. Geochronol. 50, 29–46.

Dickinson, M.R., Scott, K., Adams, N.F., Lister, A.M., Penkman, K.E.H., 2024. Amino acid dating of Pleistocene Mammalian enamel from the river thames terrace sequence: a multi-taxon approach. Quat. Geochronol. 82, 101543.

Fordham, D.A., Jackson, S.T., Brown, S.C., Huntley, B., Brook, B.W., Dahl-Jensen, D., Gilbert, M.T.P., Otto-Bliesner, B.L., Svensson, A., Theodoridis, S., Wilmshurst, J.M., Buettel, J.C., Canteri, E., McDowell, M., Orlando, L., Pilowsky, J.A., Rahbek, C., Nogues-Bravo, D., 2020. Using paleo-archives to safeguard biodiversity under climate change. Science 369, eabc5654.

Kaufman, D.S., Manley, W.F., 1998. A new procedure for determining dl amino acid ratios in fossils using reverse phase liquid chromatography. Quat. Sci. Rev. 17, 987–1000.

Kugimiya, A., Wakimoto, S., Kohda, J., Nakano, Y., Takano, Y., 2022. Development of a one-step analysis method for several amino acids using a microfluidic paper-based analytical device. Sci. Rep. 12.

Li, Z., Bai, Y., You, M., Hu, J., Yao, C., Cao, L., Xu, F., 2021. Fully integrated microfluidic devices for qualitative, quantitative and digital nucleic acids testing at point of care. Biosens. Bioelectron. 177, 112952.

Manz, A., Neužil, P., O'Connor, J.S., Simone, G., 2020. Microfluidics and Lab-on-a-Chip. The Royal Society of Chemistry.

Parton, J., Abu-Mandil Hassan, N., Brown, T.A., Haswell, S.J., Brown, K.A., Shaw, K.J., 2012. Sex identification of ancient DNA samples using a microfluidic device. J. Archaeol. Sci. 40, 705–711.

Paterson, R.S., Mackie, M., Capobianco, A., Heckeberg, N.S., Fraser, D., Munir, F., Patramanis, I., Ramos-Madrigal, J., Liu, S., Ramsøe, A.D., Dickinson, M.R., Baldreki, C., Gilbert, M., Sardella, R., Bellucci, L., Scorrano, G., Racimo, F., Willerslev, E., Penkman, K.E.H., Olsen, J.V., MacPhee, R.D.E., Rybczynski, N., Höhna, S., Cappellini, E., 2024. A 20+ Ma old enamel proteome from Canada's high arctic reveals diversification of rhinocerotidae in the middle Eocene-Oligocene. bioRxiv, 597871, 2024.2006.2007.

Penkman, K.E.H., Kaufman, D.S., Maddy, D., Collins, M.J., 2008. Closed-system behaviour of the intra-crystalline fraction of amino acids in mollusc shells. Quat. Geochronol. 3, 2–25.

Pietrogrande, M.C., 2013. Enantioselective separation of amino acids as biomarkers indicating life in extraterrestrial environments amino acid analysis. Anal. Bioanal. Chem. 405, 7931–7940.

Politt, S.S., Pribliczki, H., Dickinson, M.R., Andersen, N., Henderson, A., Morris, D., Makarewicz, C.A., Penkman, K., Ecker, M., 2025. Insights into the middle Pleistocene fauna of South Africa: zooarchaeology, stable isotopes and dating of pniel 6. J. Quat. Sci. 1–20.

Pumera, M., 2007. Microfluidics in amino acid analysis. Electrophoresis 28, 2113–2124.

Santhosh, M., Park, T., 2022. Semi-enclosed paper sensor for highly sensitive and selective detection of proline. Anal. Chim. Acta 1231.

Song, Y., Takatsuki, K., Isokawa, M., Sekiguchi, T., Mizuno, J., Funatsu, T., Shoji, S., Tsunoda, M., 2013. Fast and quantitative analysis of branched-chain amino acids in biological samples using a pillar array column amino acid analysis. Anal. Bioanal. Chem. 405, 7993–7999.

Sykes, G.A., Collins, M.J., Walton, D.I., 1995. The significance of a geochemically isolated intracrystalline organic fraction within biominerals. Org. Geochem. 23, 1059–1065.

Vanapalli, S.A., Iacovella, C.R., Sung, K.E., Mukhija, D., Millunchick, J.M., Burns, M.A., Glotzer, S.C., Solomon, M.J., 2008. Fluidic assembly and packing of microspheres in confined channels. Langmuir 24, 3661–3670.

Whitesides, G.M., 2006. The origins and the future of microfluidics. Nature 442, 368–373.

Yin, J., Suo, Y., Zou, Z., Sun, J., Zhang, S., Wang, B., Xu, Y., Darland, D., Zhao, J.X., Mu, Y., 2019. Integrated microfluidic systems with sample preparation and nucleic acid amplification. Lab Chip 19, 2769–2785.